STACKED SEARCH FOR GRAVITATIONAL WAVES FROM THE 2006 SGR 1900+14 STORM

B. P. Abbott[1], R. Abbott[1], R. Adhikari[1], P. Ajith[2], B. Allen[2,3], G. Allen[4], R. S. Amin[5], S. B. Anderson[1],
W. G. Anderson[3], M. A. Arain[6], M. Araya[1], H. Armandula[1], P. Armor[3], Y. Aso[1], S. Aston[7], P. Aufmuth[8], C. Aulbert[2],
S. Babak[9], P. Baker[10], S. Ballmer[1], C. Barker[11], D. Barker[11], B. Barr[12], P. Barriga[13], L. Barsotti[14], M. A. Barton[1],
I. Bartos[15], R. Bassiri[12], M. Bastarrika[12], B. Behnke[9], M. Benacquista[16], J. Betzwieser[1], P. T. Beyersdorf[17],
I. A. Bilenko[18], G. Billingsley[1], R. Biswas[3], E. Black[1], J. K. Blackburn[1], L. Blackburn[14], D. Blair[13], B. Bland[11],
T. P. Bodiya[14], L. Bogue[19], R. Bork[1], V. Boschi[1], S. Bose[20], P. R. Brady[3], V. B. Braginsky[18], J. E. Brau[21], D. O. Bridges[19],
M. Brinkmann[2], A. F. Brooks[1], D. A. Brown[22], A. Brummit[23], G. Brunet[14], A. Bullington[4], A. Buonanno[24],
O. Burmeister[2], R. L. Byer[4], L. Cadonati[25], J. B. Camp[26], J. Cannizzo[26], K. C. Cannon[1], J. Cao[14], L. Cardenas[1],
S. Caride[27], G. Castaldi[28], S. Caudill[5], M. Cavaglià[29], C. Cepeda[1], T. Chalermsongsak[1], E. Chalkley[12], P. Charlton[30],
S. Chatterji[1], S. Chelkowski[7], Y. Chen[9,31], N. Christensen[32], C. T. Y. Chung[33], D. Clark[4], J. Clark[34], J. H. Clayton[3],
T. Cokelaer[34], C. N. Colacino[35], R. Conte[36], D. Cook[11], T. R. C. Corbitt[14], N. Cornish[10], D. Coward[13], D. C. Coyne[1],
J. D. E. Creighton[3], T. D. Creighton[16], A. M. Cruise[7], R. M. Culter[7], A. Cumming[12], L. Cunningham[12], S. L. Danilishin[18],
K. Danzmann[2,8], B. Daudert[1], G. Davies[34], E. J. Daw[37], D. DeBra[4], J. Degallaix[2], V. Dergachev[27], S. Desai[38],
R. DeSalvo[1], S. Dhurandhar[39], M. Díaz[16], A. Dietz[34], F. Donovan[14], K. L. Dooley[6], E. E. Doomes[40], R. W. P. Drever[41],
J. Dueck[2], I. Duke[14], J.-C. Dumas[13], J. G. Dwyer[15], C. Echols[1], M. Edgar[12], A. Effler[11], P. Ehrens[1], E. Espinoza[1],
T. Etzel[1], M. Evans[14], T. Evans[19], S. Fairhurst[34], Y. Faltas[6], Y. Fan[13], D. Fazi[1], H. Fehrmann[2], L. S. Finn[38], K. Flasch[3],
S. Foley[14], C. Forrest[42], N. Fotopoulos[3], A. Franzen[8], M. Frede[2], M. Frei[43], Z. Frei[35], A. Freise[7], R. Frey[21], T. Fricke[19],
P. Fritschel[14], V. V. Frolov[19], M. Fyffe[19], V. Galdi[28], J. A. Garofoli[22], I. Gholami[9], J. A. Giaime[19,5], S. Giampanis[2],
K. D. Giardina[19], K. Goda[14], E. Goetz[27], L. M. Goggin[3], G. González[5], M. L. Gorodetsky[18], S. Gossler[2], R. Gouaty[5],
A. Grant[12], S. Gras[13], C. Gray[11], M. Gray[44], R. J. S. Greenhalgh[23], A. M. Gretarsson[45], F. Grimaldi[14], R. Grosso[16],
H. Grote[2], S. Grunewald[9], M. Guenther[11], E. K. Gustafson[1], R. Gustafson[27], B. Hage[8], J. M. Hallam[7], D. Hammer[3],
G. D. Hammond[12], C. Hanna[1], J. Hanson[19], J. Harms[46], G. M. Harry[14], I. W. Harry[34], E. D. Harstad[21], K. Haughian[12],
K. Hayama[16], J. Heefner[1], I. S. Heng[12], A. Heptonstall[1], M. Hewitson[2], S. Hild[7], E. Hirose[22], D. Hoak[19], K. A. Hodge[1],
K. Holt[19], D. J. Hosken[47], J. Hough[12], D. Hoyland[13], B. Hughey[14], S. H. Huttner[12], D. R. Ingram[11], T. Isogai[32], M. Ito[21],
A. Ivanov[1], B. Johnson[11], W. W. Johnson[5], D. I. Jones[48], G. Jones[34], R. Jones[12], L. Ju[13], P. Kalmus[1], V. Kalogera[49],
S. Kandhasamy[46], J. Kanner[24], D. Kasprzyk[7], E. Katsavounidis[14], K. Kawabe[11], S. Kawamura[50], F. Kawazoe[2],
W. Kells[1], D. G. Keppel[1], A. Khalaidovski[2], F. Y. Khalili[18], R. Khan[15], E. Khazanov[51], P. King[1], J. S. Kissel[5],
S. Klimenko[6], K. Kokeyama[50], V. Kondrashov[1], R. Kopparapu[38], S. Koranda[3], D. Kozak[1], B. Krishnan[9], R. Kumar[12],
P. Kwee[8], P. K. Lam[44], M. Landry[11], B. Lantz[4], A. Lazzarini[1], H. Lei[16], M. Lei[1], N. Leindecker[4], I. Leonor[21], C. Li[31],
H. Lin[6], P. E. Lindquist[1], T. B. Littenberg[10], N. A. Lockerbie[52], D. Lodhia[7], M. Longo[28], M. Lormand[19], P. Lu[4],
M. Lubinski[11], A. Lucianetti[6], H. Lück[2,8], B. Machenschalk[9], M. MacInnis[14], M. Mageswaran[1], K. Mailand[1],
I. Mandel[49], V. Mandic[46], S. Márka[15], Z. Márka[15], A. Markosyan[4], J. Markowitz[14], E. Maros[1], I. W. Martin[12],
R. M. Martin[6], J. N. Marx[1], K. Mason[14], F. Matichard[5], L. Matone[15], R. A. Matzner[43], N. Mavalvala[14], R. McCarthy[11],
D. E. McClelland[44], S. C. McGuire[40], M. McHugh[53], G. McIntyre[1], D. J. A. McKechan[34], K. McKenzie[44], M. Mehmet[2],
A. Melatos[33], A. C. Melissinos[42], D. F. Menéndez[38], G. Mendell[11], R. A. Mercer[3], S. Meshkov[1], C. Messenger[2],
M. S. Meyer[19], J. Miller[12], J. Minelli[38], Y. Mino[31], V. P. Mitrofanov[18], G. Mitselmakher[6], R. Mittleman[14],
O. Miyakawa[1], B. Moe[3], S. D. Mohanty[16], S. R. P. Mohapatra[25], G. Moreno[11], T. Morioka[50], K. Mors[2], K. Mossavi[2],
C. MowLowry[44], G. Mueller[6], H. Müller-Ebhardt[2], D. Muhammad[19], S. Mukherjee[16], H. Mukhopadhyay[39],
A. Mullavey[44], J. Munch[47], P. G. Murray[12], E. Myers[11], J. Myers[11], T. Nash[1], J. Nelson[12], G. Newton[12], A. Nishizawa[50],
K. Numata[26], J. O'Dell[23], B. O'Reilly[19], R. O'Shaughnessy[38], E. Ochsner[24], G. H. Ogin[1], D. J. Ottaway[47], R. S. Ottens[6],
H. Overmier[19], B. J. Owen[38], Y. Pan[24], C. Pankow[6], M. A. Papa[9,3], V. Parameshwaraiah[11], P. Patel[1], M. Pedraza[1],
S. Penn[54], A. Perreca[7], V. Pierro[28], I. M. Pinto[28], M. Pitkin[12], H. J. Pletsch[2], M. V. Plissi[12], F. Postiglione[36],
M. Principe[28], R. Prix[2], L. Prokhorov[18], O. Punken[2], V. Quetschke[6], F. J. Raab[11], D. S. Rabeling[44], H. Radkins[11],
P. Raffai[35], Z. Raics[15], N. Rainer[2], M. Rakhmanov[16], V. Raymond[49], C. M. Reed[11], T. Reed[55], H. Rehbein[2], S. Reid[12],
D. H. Reitze[6], R. Riesen[19], K. Riles[27], B. Rivera[11], P. Roberts[56], N. A. Robertson[1,12], C. Robinson[34], E. L. Robinson[9],
S. Roddy[19], C. Röver[2], J. Rollins[15], J. D. Romano[16], J. H. Romie[19], S. Rowan[12], A. Rüdiger[2], P. Russell[1], K. Ryan[11],
S. Sakata[50], L. Sancho de la Jordana[57], V. Sandberg[11], V. Sannibale[1], L. Santamaría[9], S. Saraf[58], P. Sarin[14],
B. S. Sathyaprakash[34], S. Sato[50], M. Satterthwaite[44], P. R. Saulson[22], R. Savage[11], P. Savov[31], M. Scanlan[55],
R. Schilling[2], R. Schnabel[2], R. Schofield[21], B. Schulz[2], B. F. Schutz[9,34], P. Schwinberg[11], J. Scott[12], S. M. Scott[44],
A. C. Searle[1], B. Sears[1], F. Seifert[2], D. Sellers[19], A. S. Sengupta[1], A. Sergeev[51], B. Shapiro[14], P. Shawhan[24],
D. H. Shoemaker[14], A. Sibley[19], X. Siemens[3], D. Sigg[11], S. Sinha[4], A. M. Sintes[57], B. J. J. Slagmolen[44], J. Slutsky[5],
J. R. Smith[22], M. R. Smith[1], N. D. Smith[14], K. Somiya[31], B. Sorazu[12], A. Stein[14], L. C. Stein[14], S. Steplewski[20],
A. Stochino[1], R. Stone[16], K. A. Strain[12], S. Strigin[18], A. Stroeer[26], A. L. Stuver[19], T. Z. Summerscales[56], K.-X. Sun[4],
M. Sung[5], P. J. Sutton[34], G. P. Szokoly[35], D. Talukder[20], L. Tang[16], D. B. Tanner[6], S. P. Tarabrin[18], J. R. Taylor[2],
R. Taylor[1], J. Thacker[19], K. A. Thorne[19], K. S. Thorne[31], A. Thüring[8], K. V. Tokmakov[12], C. Torres[19], C. Torrie[1],

G. Traylor[19], M. Trias[57], D. Ugolini[59], J. Ulmen[4], K. Urbanek[4], H. Vahlbruch[8], M. Vallisneri[31], C. van den Broeck[34],
M. V. van der Sluys[49], A. A. van Veggel[12], S. Vass[1], R. Vaulin[3], A. Vecchio[7], J. Veitch[7], P. Veitch[47], C. Veltkamp[2],
A. Villar[1], C. Vorvick[11], S. P. Vyachanin[18], S. J. Waldman[14], L. Wallace[1], R. L. Ward[1], A. Weidner[2], M. Weinert[2],
A. J. Weinstein[1], R. Weiss[14], L. Wen[31,13], S. Wen[5], K. Wette[44], J. T. Whelan[9,60], S. E. Whitcomb[1], B. F. Whiting[6],
C. Wilkinson[11], P. A. Willems[1], H. R. Williams[38], L. Williams[6], B. Willke[2,8], I. Wilmut[23], L. Winkelmann[2],
W. Winkler[2], C. C. Wipf[14], A. G. Wiseman[3], G. Woan[12], R. Wooley[19], J. Worden[11], W. Wu[6], I. Yakushin[19],
H. Yamamoto[1], Z. Yan[13], S. Yoshida[61], M. Zanolin[45], J. Zhang[27], L. Zhang[1], C. Zhao[13], N. Zotov[55], M. E. Zucker[14],
H. zur Mühlen[8], and J. Zweizig[1]

(The LIGO Scientific Collaboration[62])

[1] LIGO - California Institute of Technology, Pasadena, CA 91125, USA
[2] Albert-Einstein-Institut, Max-Planck-Institut für Gravitationsphysik, D-30167 Hannover, Germany
[3] University of Wisconsin–Milwaukee, Milwaukee, WI 53201, USA
[4] Stanford University, Stanford, CA 94305, USA
[5] Louisiana State University, Baton Rouge, LA 70803, USA
[6] University of Florida, Gainesville, FL 32611, USA
[7] University of Birmingham, Birmingham B15 2TT, UK
[8] Leibniz Universität Hannover, D-30167 Hannover, Germany
[9] Albert-Einstein-Institut, Max-Planck-Institut für Gravitationsphysik, D-14476 Golm, Germany
[10] Montana State University, Bozeman, MT 59717, USA
[11] LIGO - Hanford Observatory, Richland, WA 99352, USA
[12] University of Glasgow, Glasgow G12 8QQ, UK
[13] University of Western Australia, Crawley, WA 6009, Australia
[14] LIGO - Massachusetts Institute of Technology, Cambridge, MA 02139, USA
[15] Columbia University, New York, NY 10027, USA
[16] The University of Texas at Brownsville and Texas Southmost College, Brownsville, TX 78520, USA
[17] San Jose State University, San Jose, CA 95192, USA
[18] Moscow State University, Moscow 119992, Russia
[19] LIGO - Livingston Observatory, Livingston, LA 70754, USA
[20] Washington State University, Pullman, WA 99164, USA
[21] University of Oregon, Eugene, OR 97403, USA
[22] Syracuse University, Syracuse, NY 13244, USA
[23] Rutherford Appleton Laboratory, HSIC, Chilton, Didcot, Oxon OX11 0QX, UK
[24] University of Maryland, College Park, MD 20742, USA
[25] University of Massachusetts, Amherst, MA 01003, USA
[26] NASA/Goddard Space Flight Center, Greenbelt, MD 20771, USA
[27] University of Michigan, Ann Arbor, MI 48109, USA
[28] University of Sannio at Benevento, I-82100 Benevento, Italy
[29] The University of Mississippi, University, MS 38677, USA
[30] Charles Sturt University, Wagga Wagga, NSW 2678, Australia
[31] Caltech-CaRT, Pasadena, CA 91125, USA
[32] Carleton College, Northfield, MN 55057, USA
[33] The University of Melbourne, Parkville, VIC 3010, Australia
[34] Cardiff University, Cardiff CF24 3AA, UK
[35] Eötvös University, ELTE 1053 Budapest, Hungary
[36] University of Salerno, 84084 Fisciano (Salerno), Italy
[37] The University of Sheffield, Sheffield S10 2TN, UK
[38] The Pennsylvania State University, University Park, PA 16802, USA
[39] Inter-University Centre for Astronomy and Astrophysics, Pune 411007, India
[40] Southern University and A&M College, Baton Rouge, LA 70813, USA
[41] California Institute of Technology, Pasadena, CA 91125, USA
[42] University of Rochester, Rochester, NY 14627, USA
[43] The University of Texas at Austin, TX 78712, USA
[44] Australian National University, Canberra 0200, Australia
[45] Embry-Riddle Aeronautical University, Prescott, AZ 86301, USA
[46] University of Minnesota, Minneapolis, MN 55455, USA
[47] University of Adelaide, Adelaide, SA 5005, Australia
[48] University of Southampton, Southampton SO17 1BJ, UK
[49] Northwestern University, Evanston, IL 60208, USA
[50] National Astronomical Observatory of Japan, Tokyo 181-8588, Japan
[51] Institute of Applied Physics, Nizhny Novgorod 603950, Russia
[52] University of Strathclyde, Glasgow G1 1XQ, UK
[53] Loyola University, New Orleans, LA 70118, USA
[54] Hobart and William Smith Colleges, Geneva, NY 14456, USA
[55] Louisiana Tech University, Ruston, LA 71272, USA
[56] Andrews University, Berrien Springs, MI 49104, USA
[57] Universitat de les Illes Balears, E-07122 Palma de Mallorca, Spain
[58] Sonoma State University, Rohnert Park, CA 94928, USA
[59] Trinity University, San Antonio, TX 78212, USA
[60] Rochester Institute of Technology, Rochester, NY 14623, USA
[61] Southeastern Louisiana University, Hammond, LA 70402, USA

ABSTRACT

We present the results of a LIGO search for short-duration gravitational waves (GWs) associated with the 2006 March 29 SGR 1900+14 storm. A new search method is used, "stacking" the GW data around the times of individual soft-gamma bursts in the storm to enhance sensitivity for models in which multiple bursts are accompanied by GW emission. We assume that variation in the time difference between burst electromagnetic emission and potential burst GW emission is small relative to the GW signal duration, and we time-align GW excess power time–frequency tilings containing individual burst triggers to their corresponding electromagnetic emissions. We use two GW emission models in our search: a fluence-weighted model and a flat (unweighted) model for the most electromagnetically energetic bursts. We find no evidence of GWs associated with either model. Model-dependent GW strain, isotropic GW emission energy $E_{\rm GW}$, and $\gamma \equiv E_{\rm GW}/E_{\rm EM}$ upper limits are estimated using a variety of assumed waveforms. The stacking method allows us to set the most stringent model-dependent limits on transient GW strain published to date. We find $E_{\rm GW}$ upper limit estimates (at a nominal distance of 10 kpc) of between 2×10^{45} erg and 6×10^{50} erg depending on the waveform type. These limits are an order of magnitude lower than upper limits published previously for this storm and overlap with the range of electromagnetic energies emitted in soft gamma repeater (SGR) giant flares.

Key words: gamma rays: bursts – gravitational waves – pulsars: individual (SGR 1900+14) – stars: neutron

1. INTRODUCTION

Soft gamma repeaters (SGRs) sporadically emit brief (~ 0.1 s) intense bursts of soft gamma-rays. Three of the five known SGRs have produced rare "giant flare" events with initial bright, short (~ 0.2 s) pulses with peak electromagnetic (EM) luminosities between 10^{44} and 10^{47} erg s^{-1}, placing them among the most EM luminous events in the universe. According to the "magnetar" model SGRs are galactic neutron stars with extreme magnetic fields $\sim 10^{15}$ G (Duncan & Thompson 1992). Bursts may result from the interaction of the star's magnetic field with its solid crust, leading to crustal deformations and occasional catastrophic cracking (Thompson & Duncan 1995; Schwartz et al. 2005; Horowitz & Kadau 2009) with subsequent excitation of nonradial neutron star f-modes (Andersson & Kokkotas 1998; de Freitas Pacheco 1998; Ioka 2001) and the emission of GWs (de Freitas Pacheco 1998; Ioka 2001; Horvath 2005; Owen 2005). For reviews, see Mereghetti (2008) and Woods & Thompson (2004).

Occasionally, SGRs produce many soft gamma bursts in a brief period of time; such intense emissions are referred to as "storms." We present a search for short-duration GW signals ($\lesssim 0.3$ s) associated with *multiple* bursts in the 2006 March 29 SGR 1900+14 storm (Israel et al. 2008) using data collected by the Laser Interferometer Gravitational Wave Observatory (LIGO; Abbott et al. 2009b). The storm light curve, obtained from the Burst Alert Telescope (BAT) aboard the *Swift* satellite (Barthelmy et al. 2005), is shown in Figure 1. It consists of more than 40 bursts in $\sim$30 s, including common SGR bursts and some intermediate flares with durations > 0.5 s. The total fluence for the storm event was estimated by the Konus-Wind team to be $(1–2) \times 10^{-4}$ erg cm^{-2} in the (20–200) keV range (Golenetskii et al. 2006), implying an isotropic EM energy $E_{\rm EM} = (1–2) \times 10^{42}$ erg at a nominal distance to SGR 1900+14 of 10 kpc (source location and distance is discussed in Kaplan et al. 2002). At the time of the storm both of the 4 km LIGO detectors (located at Hanford, WA and Livingston, LA) were taking science quality data.

We attempt to improve sensitivity to multiple weak GW burst signals associated with the storm's multiple EM bursts by adding

together GW signal power over multiple bursts. In doing so we assume particular GW emission models, which we describe in the next section. Figure 2 illustrates the stacking procedure using the four most energetic bursts in the storm.

2. METHODS

The analysis is performed by the Stack-a-flare pipeline (Kalmus et al. 2009), which extends the method used in a recent LIGO search for transient GW associated with individual SGR bursts (Abbott et al. 2008a) and relies on an excess power detection statistic (Anderson et al. 2001). To "stack" N bursts in the storm, we first generate N excess power time–frequency tilings. These are two-dimensional matrices in time and frequency produced by combining the two detectors' data streams so as to provide sensitivity to correlated signals, as described in Kalmus et al. (2007). Each tiling element gives an excess power estimate in the GW detector data stream in a small period of time δt and a small range of frequency δf. The time range of each tiling is chosen to be centered on the time of one of the target EM bursts in the storm. We then align these N tilings along the time dimension so that times of the target EM bursts coincide, and perform a weighted addition.

Stacking significantly improves sensitivity to GW emission under a given model. However, improving detection probability depends upon stacking according to GW emission models that correctly describe nature. The storm light curve motivated two stacking models: a flat-weighted model with an energy cutoff, which includes the 11 most energetic EM bursts with unity weighting factors; and an EM-fluence-weighted model comprised of the 18 most energetic EM bursts. In the flat model, we assume that a fixed amount of GW energy is released in each burst independently of its EM energy, provided the EM energy is above a threshold. The threshold choice is motivated by a clear separation in EM fluence of the 11 most energetic bursts from out of the total of $\sim$40 bursts in the storm observed by BAT. A histogram of EM fluence of bursts (in terms of BAT counts) illustrating this separation is shown in Kalmus et al. (2009). In the EM-fluence-weighted model, we make the hypothesis that $\gamma \equiv E_{\rm GW}/E_{\rm EM}$ is constant from burst to burst, i.e., $E_{\rm GW}$ is always proportional to $E_{\rm EM}$. Including the 18 most energetic bursts accounts for 95% of the total EM fluence of the more
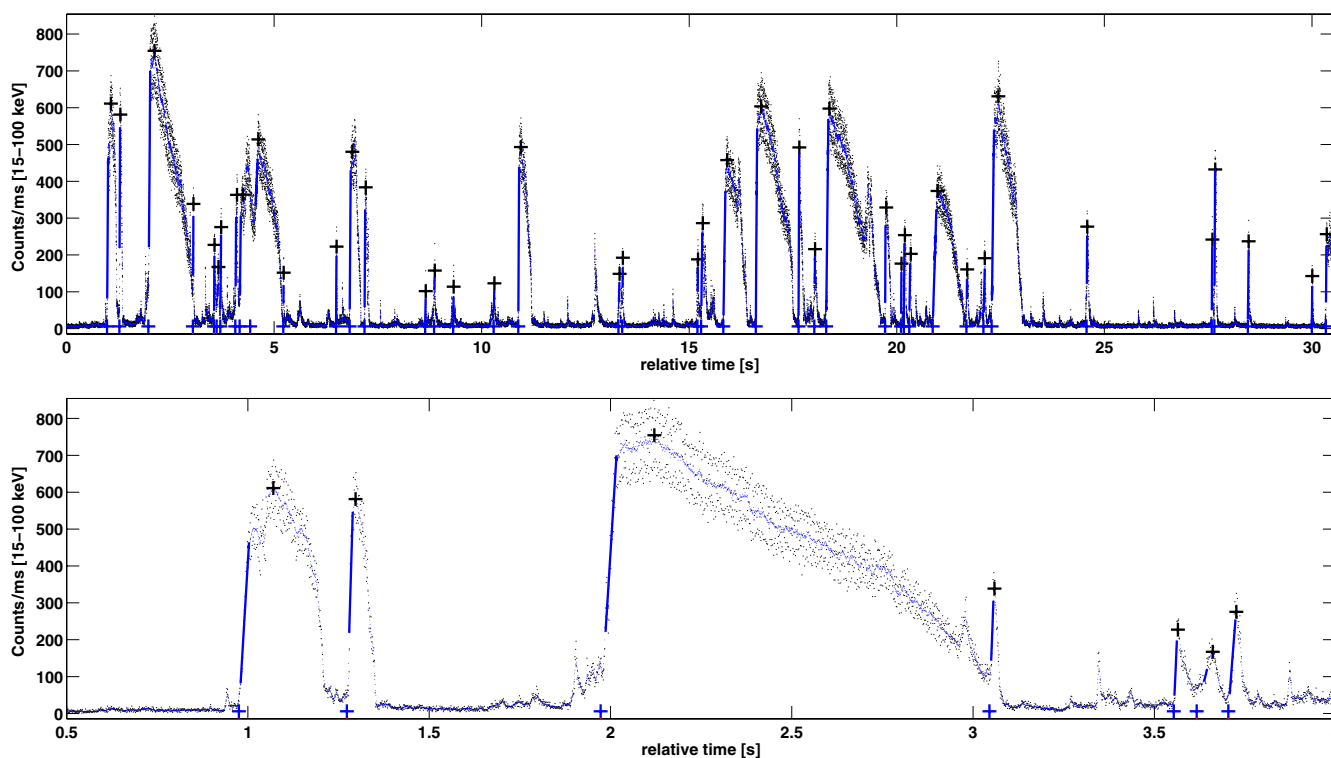
Figure 1. SGR 1900+14 storm light curve with 1 ms bins as seen by the *Swift* BAT detector in the (15–100) keV band (Barthelmy et al. 2005). Bottom plot shows a detail. Burst start times are estimated by fitting the steeply rising burst edges; EM fluences are estimated by integrating light curve area under each burst. A 30 bin running average is shown in addition to the raw light curve. Solid lines are linear fits to rising edges; the boundaries of rising edges were found by examining the first derivatives in the neighborhoods of the peak locations. Crosses mark burst peaks and intersections of the rising edge fits extrapolated to a linear fit of the noise floor measured in a quiescent period of data in the 50 s BAT sequence before the start of the storm. The one-sigma timing uncertainty averaged over all measurements is 2.9 ms. *X*-axis times are relative to 2006 March 29 02:53:09.9 UT at the *Swift* satellite.
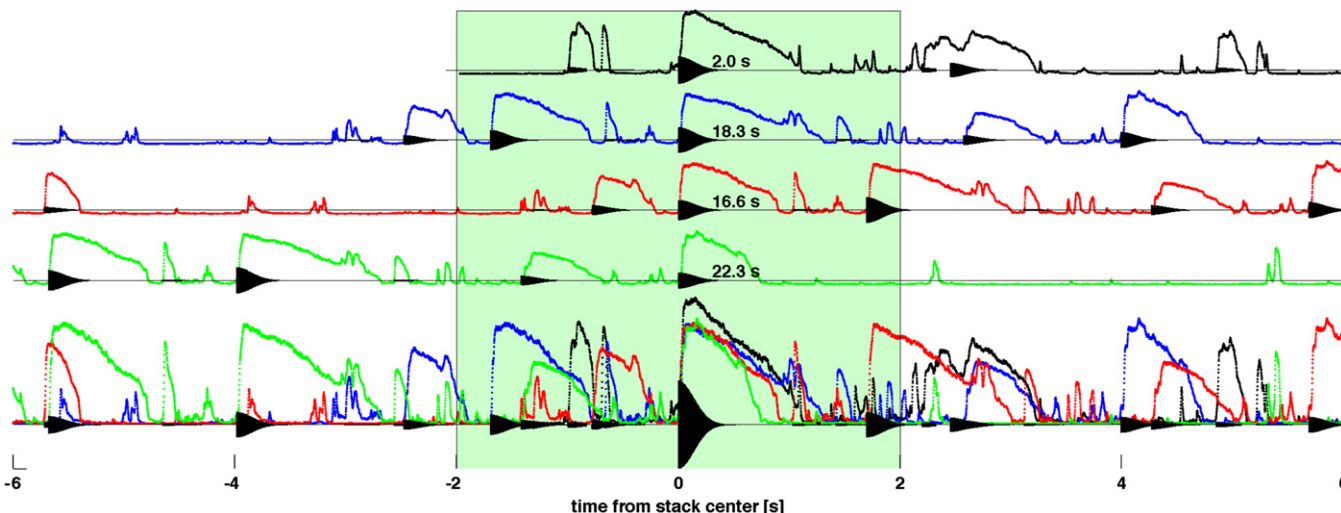
Figure 2. Individual EM bursts inform the stacking of GW data. This figure suggests the stacking procedure and explicitly shows search timescales. The top four plots are EM light curve time series around individual bursts beginning at 2.0 s, 16.6 s, 18.3 s, and 22.3 s in Figure 1. Simulated GW ringdowns in the fluence-weighted model are superposed. The bottom plot shows the EM time series simultaneously, and the sum of the hypothetical GW signals. The on-source region of ±2 s is shaded. In the search, GW data corresponding to the EM time series are transformed to time–frequency power tilings before being added together and therefore there is no dependence on phase-coherence of GW signals in the analysis; this transformation is not illustrated.

than 40 bursts in the light curve. Both burst samples include the seven intermediate flares identified in Israel et al. (2008). In the fluence-weighted model, time–frequency excess power tilings are weighted according to burst-integrated BAT counts before stacking. Further details are in Kalmus et al. (2009).

To obtain estimates of the times of EM bursts in the storm, we measure the intersections of the rapid rising edges of each burst with the light curve noise floor measured in a quiescent period of data in the 50 s BAT sequence before the start of the storm (Figure 1). We correct these times for satellite-to-geocenter times-of-flight using the known SGR 1900+14 sky position and *Swift* ephemeris, which vary from (17.12 to 17.48) ms over the ~30 s duration of the storm. The stack-a-flare analysis method is robust to relative timing errors smaller than

GW signal durations (Kalmus et al. 2009). EM fluences are estimated by integrating detector counts under each burst in the light curve. We conservatively converted counts to fluences using the lower bound of the Konus-Wind total fluence range given above, making the assumption that burst spectra are constant from burst to burst.

We divide the GW data into an on-source time region, in which GWs associated with the storm could be expected, and a background region, with statistically similar noise in which we do not expect a GW. This is done after data quality cuts (categories 1 and 2 described in Abbott et al. 2009a) are applied to the GW data, so as to remove, e.g., periods of instrumental or data acquisition problems, or nonstationary noise due to bad weather or other environmental conditions. The on-source region consists of 4 s of stacked data. Each 4 s region comprising the stack is centered on the time of one of the EM bursts included in the GW emission stacking model. Background regions consist of 1000 s of data on either side of the storm. On-source and background segments are analyzed and stacked identically, and the stacked time–frequency tilings are passed through a two-dimensional clustering algorithm resulting in lists of "analysis events." Each analysis event corresponds to one discrete cluster found by the algorithm and consists of information on the cluster central frequency, central time, bandwidth, and duration (Kalmus et al. 2009). Background analysis events due to fluctuating detector noise are used to estimate the significance of on-source events; significant events, if any, are subject to vetoes (Abbott et al. 2009a).

Using ±2 s regions around bursts in the storm accounts for uncertainties in the EM burst times and a possible systematic delay between GW and EM emission. Although GW emission in SGRs is expected to occur almost simultaneously with the EM burst (Ioka 2001), a common bias in trigger times shared by all bursts in the stacking set of $\lesssim 1$ s can be handled with a ±2 s on-source region.

As in Abbott et al. (2008a), this search targets neutron star fundamental mode ringdowns (RDs) predicted in Andersson & Kokkotas (1998), de Freitas Pacheco (1998), Ioka (2001), and Andersson (2003) as well as short-duration GW signals of unknown waveform. RDs are targeted because f-modes are the most efficient GW emitters (Andersson & Kokkotas 1998). We assume that given a neutron star, f-mode frequencies and damping timescales would be similar from event to event, and that unknown signals would at least have similar central frequencies and durations from event to event.

As in Abbott et al. (2008a), we thus focus on two distinct regions in the target signal time–frequency parameter space. The first region targets ∼100–400 ms duration signals in the (1–3) kHz band, which includes f-mode RD signals predicted in Benhar et al. (2004) for ten realistic neutron star equations of state. We choose a search band of (1–3) kHz for RD searches, with a 250 ms time window which was found to give optimal search sensitivity (Kalmus 2008). The second region targets ∼(5–200) ms duration signals in the (100–1000) Hz band. The target durations are set by prompt SGR burst timescales (5–200 ms) and the target frequencies are set by the detector's sensitive region. We search in two bands: (100–200) Hz (probing the region in which the detectors are most sensitive) and (100–1000) Hz (for full spectral coverage below the RD search band) using a 125 ms time window. In all, we search in three frequency bands and two GW emission models (flat and fluence-weighted). This amounts to a total of six 4 s long stacked on-source regions.

We estimate loudest-event upper limits (Brady et al. 2004) on GW root-sum-squared strain $h_{\rm rss}$ incident at the detector. We can construct simulations of impinging GW with a given $h_{\rm rss}$. Following Abbott et al. (2005b)

$$h_{\rm rss}^2 = h_{\rm rss+}^2 + h_{\rm rss\times}^2, \tag{1}$$

where, e.g.,

$$h_{\rm rss+}^2 = \int_{-\infty}^{\infty} |h_+|^2 \, dt \tag{2}$$

and $h_{+,\times}(t)$ are the two GW polarizations. The relationship between the GW polarizations and the detector response $h(t)$ to an impinging GW from a polar angle and azimuth (θ, ϕ) and with polarization angle ψ is

$$h(t) = F_+(\theta, \phi, \psi)h_+(t) + F_\times(\theta, \phi, \psi)h_\times(t), \tag{3}$$

where $F_+(\theta, \phi, \psi)$ and $F_\times(\theta, \phi, \psi)$ are the antenna functions for the source at (θ, ϕ) (Thorne 1987). At the time of the storm, the polarization-independent rms antenna response $(F_+^2 + F_\times^2)^{1/2}$, which indicates the average sensitivity to a given sky location, was 0.39 for LIGO Hanford observatory and 0.46 for the LIGO Livingston observatory.

We can also set upper limits on the emitted isotropic GW emission energy $E_{\rm GW}$ at a source distance R associated with $h_+(t)$ and $h_\times(t)$ via (Shapiro & Teukolsky 1983)

$$E_{\rm GW} = 4\pi R^2 \frac{c^3}{16\pi G} \int_{-\infty}^{\infty} ((\dot{h}_+)^2 + (\dot{h}_\times)^2) dt. \tag{4}$$

The procedure for estimating loudest-event upper limits in the individual burst search is detailed in Kalmus (2008), Abbott et al. (2008a), and Acernese et al. (2008). In brief, the upper limit is computed in a frequentist framework by injecting artificial signals into the background data and recovering them with the search pipeline (see for example Abbott et al. 2005a, 2008b). An analysis event is associated with each injection, and compared to the loudest on-source analysis event. The GW strain or isotropic energy at 90% detection efficiency is the strain or isotropic energy at which 90% of injections have associated events louder than the loudest on-source event.

We use the 12 waveform types described in Abbott et al. (2008a) to establish detector sensitivity and thereby set upper limits: linearly and circularly polarized RDs with $\tau = 200$ ms and frequencies in the range (1–3) kHz; and band- and time-limited white noise bursts (WNBs) with durations of 11 ms and 100 ms and frequency bands matched to the two lower frequency search bands.

These waveforms are used to construct compound injections determined by the emission model. In the flat model, 11 GW bursts comprise a compound injection, each is identical, and our stated $h_{\rm rss}$ and $E_{\rm GW}$ are for one such GW burst in the compound injection. In the fluence-weighted model, 18 GW bursts comprise a compound injection, they are weighted (in amplitude) with the square root of integrated counts, and our stated $h_{\rm rss}$ and $E_{\rm GW}$ are for the loudest GW burst in the compound injection. A single polarization angle is chosen randomly for every compound injection. In assuming that the bursts emitted are identical up to an amplitude scale factor, we implicitly assume that the star's GW emission mechanism and symmetry axis are constant over bursts in the storm.

Table 1
Stack-A-Flare SGR 1900+14 Storm Upper Limits

Simulation Type	N=11 Flat			N=18 Fluence-Weighted		
	$h_{\rm rss}^{90\%}[10^{-22}\,{\rm Hz}^{-\frac{1}{2}}]$	$E_{\rm GW}^{90\%}$ [erg]	$\gamma_{\rm UL}$	$h_{\rm rss}^{90\%}[10^{-22}\,{\rm Hz}^{-\frac{1}{2}}]$	$E_{\rm GW}^{90\%}$ [erg]	$\gamma_{\rm UL}$
WNB 11ms 100–200 Hz	$1.3\,^{+0.0+0.17+0.0} = 1.5$	1.9×10^{45}	3×10^{4}	$2.1\,^{+0.0+0.27+0.094} = 2.4$	5.0×10^{45}	3×10^{4}
WNB 100ms 100–200 Hz	$1.5\,^{+0.0+0.19+0.0} = 1.7$	2.4×10^{45}	4×10^{4}	$2.3\,^{+0.0+0.30+0.098} = 2.6$	6.0×10^{45}	3×10^{4}
WNB 11ms 100–1000 Hz	$3.5\,^{+0.0+0.45+0.0} = 3.9$	1.8×10^{47}	3×10^{6}	$5.2\,^{+0.0+0.67+0.29} = 5.9$	4.1×10^{47}	2×10^{6}
WNB 100ms 100–1000 Hz	$3.8\,^{+0.0+0.50+0.0} = 4.3$	2.0×10^{47}	3×10^{6}	$5.6\,^{+0.0+0.73+0.29} = 6.3$	4.5×10^{47}	2×10^{6}
RDC 200ms 1090 Hz	$4.5\,^{+0.045+0.59+0.0} = 5.2$	1.2×10^{48}	2×10^{7}	$7.2\,^{+0.072+0.93+0.33} = 8.2$	3.0×10^{48}	2×10^{7}
RDC 200ms 1590 Hz	$6.4\,^{+0.19+0.84+0.0} = 7.4$	5.1×10^{48}	8×10^{7}	$11\,^{+0.33+1.4+0.44} = 13$	1.5×10^{49}	8×10^{7}
RDC 200ms 2090 Hz	$9.3\,^{+0.28+1.8+0.41} = 11$	2.1×10^{49}	3×10^{8}	$14\,^{+0.43+2.8+0.72} = 18$	4.9×10^{49}	3×10^{8}
RDC 200ms 2590 Hz	$11\,^{+0.34+2.2+0.32} = 14$	4.6×10^{49}	8×10^{8}	$17\,^{+0.50+3.3+1.0} = 21$	1.0×10^{50}	5×10^{8}
RDL 200ms 1090 Hz	$9.3\,^{+0.0+1.2+0.95} = 11$	5.3×10^{48}	9×10^{7}	$16\,^{+0.0+2.1+1.6} = 18$	1.5×10^{49}	8×10^{7}
RDL 200ms 1590 Hz	$14\,^{+0.42+1.8+1.1} = 17$	2.6×10^{49}	4×10^{8}	$19\,^{+0.58+2.5+1.9} = 23$	5.1×10^{49}	3×10^{8}
RDL 200ms 2090 Hz	$20\,^{+1.2+3.9+1.4} = 25$	1.0×10^{50}	2×10^{9}	$27\,^{+1.6+5.3+2.8} = 34$	1.9×10^{50}	1×10^{9}
RDL 200ms 2590 Hz	$25\,^{+1.8+5.0+3.0} = 33$	2.6×10^{50}	4×10^{9}	$39\,^{+2.7+7.7+2.5} = 50$	6.2×10^{50}	3×10^{9}

Notes. Superscripts account for statistical and systematic errors as described in Section 3. Upper limit estimates on $\gamma \equiv E_{\rm GW}/E_{\rm EM}$ are computed assuming that spectra are constant from burst to burst, and using a BAT counts-to-fluence conversion factor estimated using the lower bound of the total fluence measured by Konus-Wind during the storm.
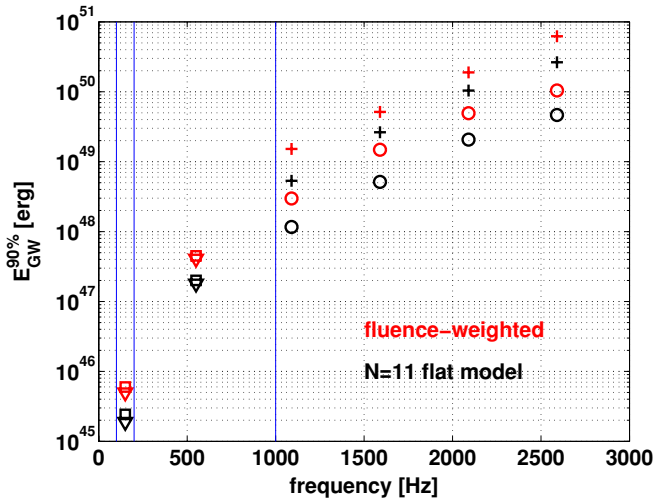
Figure 3. Stack-a-flare SGR 1900+14 storm isotropic energy upper limit estimates at 10 kpc, for flat and fluence-weighted emission models. We set upper limits at characteristic points in the signal parameter space in order to quantify the meaning of our nondetection result. Uncertainties have been folded in. Vertical lines indicate boundaries of the three distinct search frequency bands. Crosses and circles indicate linearly and circularly polarized RDs, respectively. Triangles and squares represent 11 ms and 100 ms band- and time-limited WNBs, respectively. Symbols are placed at the waveform central frequency. These results reflect the noise curves of the detectors.

3. RESULTS

We find no statistically significant GW signal associated with the SGR 1900+14 storm. The significance of on-source analysis events is inferred by noting the rate at which background analysis events of equal or greater loudness occur. We examined 4 s stacked on-source regions in the flat and fluence-weighted models in the three search bands. The most significant on-source analysis event from these six searches was from the flat model in the (100–1000) Hz band and had a corresponding background rate of 5.0×10^{-2} Hz (1 per 20 s) in that search.

Table 1 and Figure 3 give model-dependent loudest-event upper limits at 90% detection efficiency computed for the GW signal associated with the single loudest EM burst. We give strain upper limits ($h_{\rm rss}^{90\%}$) and isotropic emission energy upper limits at a nominal SGR 1900+14 distance of 10 kpc ($E_{\rm GW}^{90\%}$).

We also give upper limits $\gamma_{\rm UL} = E_{\rm GW}^{90\%}/E_{\rm EM}$, a source-distance-independent measure of the extent to which an energy upper limit probes the GW emission efficiency, calculated using a conservative estimate of 1.0×10^{-4} erg cm^{-2} for the total fluence of the storm to estimate fluences for individual peaks. In the fluence-weighted model, γ is the same for each individual burst. In the flat model, we report the mean value of γ for the 11 bursts.

Superscripts in Table 1 give a systematic error and uncertainties at 90% confidence. (Similar estimates were made for the $E_{\rm GW}^{90\%}$ but are not shown in the table.) The first and second superscripts account for the systematic error and statistical uncertainty, respectively, in the detector calibrations. The third is the statistical uncertainty from using a finite number of trials (200) in the Monte Carlos, estimated with the bootstrap method using 200 ensembles (Efron 1979). The systematic error and the quadrature sum of the statistical uncertainties are added to the final sensitivity estimates. One-sigma burst timing uncertainties from fits of burst rising edges are accounted for in the Monte Carlo simulations. Estimating uncertainties is further described in Kalmus et al. (2009).

4. DISCUSSION

The stacked search described here extends the recent LIGO search for GW associated with the 2004 SGR 1806–20 giant flare and 190 lesser events from SGR 1806–20 and SGR 1900+14 (Abbott et al. 2008a). That search was the first search sensitive to neutron star f-modes, and it set individual burst upper limits $E_{\rm GW}^{90\%}$ ranging from 3×10^{45} erg to 9×10^{52} erg (depending on the waveform type and detector antenna factors and noise characteristics at the time of the burst), but did not detect any GWs. The best values of $\gamma_{\rm UL}$ in Abbott et al. (2008a), for the giant flare, were in the range 5×10^{1}–6×10^{6} depending on the waveform type.

The upper limits obtained here are a factor of 12 more sensitive in energy than the SGR 1900+14 storm upper limits in Abbott et al. (2008a), which analyzed the storm in a single ± 20 s on-source region. Those previous limits already overlapped the range of EM energies seen in the loudest flares as well as the range of GW energies predicted by the most extreme models (Ioka 2001). The flat model gives isotropic energy upper

limits on average a factor of 4 lower than a reference $N = 1$ (nonstacked) scenario (with a ± 2 s on-source region) and a factor of 2 lower than the fluence-weighted model. However, our storm γ upper limits are still a few hundred times the SGR 1806–20 giant flare γ upper limits, due to the tremendous EM energy released by the giant flare. There is very little discussion of γ in the theory literature with which to compare.

The Advanced LIGO detectors promise an improvement in energy sensitivity of more than a factor of 100. Furthermore, on 2008 August 22, SGR 0501+4516 was discovered (Holland et al. 2008; Barthelmy et al. 2008; Palmer & Barthelmy 2008) and may be located only 1.5 kpc away (Gaensler & Chatterjee 2008; Leahy & Aschenbach 1995). SGR 0501+4516 searches will thus gain an additional 2 orders of magnitude in energy and γ upper limits compared to SGRs at 10 kpc. A stacking analysis of SGR 0501+4516 bursts with Advanced LIGO (a gain of 4 orders of magnitude in energy sensitivity) could therefore reach γ values below unity, even without another giant flare.

In the future, we plan to carry out stacking searches on both SGR storms, and also on isolated SGR bursts, as the sensitivity of detectors in the global network of GW interferometers continues to improve. For example, enhanced LIGO detectors will come online this year (2009), and data from the Virgo and GEO detectors in Europe can be used in future searches as well. Our stacked upper limits depend on theoretical guidance as to what weightings and time delays are possible, and the significance of our results depends on predictions of the range of E_{GW} and γ; yet all of these things are scarce. We hope that our continued efforts to search for GW associated with SGR and anomalous X-ray pulsar bursts encourage further modeling of GW emission from these intriguing objects.

REFERENCES

Abbott, B. P., et al. 2005a, Phys. Rev. D, 72, 082001
Abbott, B. P., et al. 2005b, Phys. Rev. D, 72, 062001
Abbott, B. P., et al. 2008a, Phys. Rev. Lett., 101, 211102
Abbott, B. P., et al. 2008b, Phys. Rev. D, 77, 062004
Abbott, B. P., et al. 2009a, arXiv:0905.0020
Abbott, B. P., et al. 2009b, Reports on Progress in Physics, 72, 076901
Acernese, F. 2008, Class. Quant. Grav., 25, 5001A
Anderson, W. G., Brady, P. R., Creighton, J. D., & Flanagan, É. É. 2001, Phys. Rev. D, 63, 042003
Andersson, N. 2003, Class. Quant. Grav., 20, 105
Andersson, N., & Kokkotas, K. D. 1998, MNRAS, 299, 1059
Barthelmy, S., et al. 2005, Space Sci. Rev., 120, 143
Barthelmy, S., et al. 2008, GCN Circ. 8113
Benhar, O., Ferrari, V., & Gualtieri, L. 2004, Phys. Rev. D, 70, 124015
Brady, P. R., Creighton, J. D. E., & Wiseman, A. G. 2004, Class. Quant. Grav., 21, S1775
de Freitas Pacheco, J. A. 1998, A&A, 336, 397
Duncan, R. C., & Thompson, C. 1992, ApJ, 392, L9
Efron, B. 1979, Ann. Stat., 7, 1
Gaensler, B. M., & Chatterjee, S. 2008, GCN Circ. 8149
Golenetskii, S., et al. 2006, GCN Circ. 4946
Holland, S. T., et al. 2008, GCN Circ. 8112
Horowitz, C. J., & Kadau, K. 2009, Phys. Rev. Lett., 102, 191102
Horvath, J. E. 2005, Mod. Phys. Lett. A, 20, 2799
Ioka, K. 2001, MNRAS, 327, 639
Israel, G. L., et al. 2008, ApJ, 685, 1114
Kalmus, P. 2008, PhD thesis, Columbia University
Kalmus, P., Cannon, K. C., Márka, S., & Owen, B. J. 2009, arXiv:0904.4906
Kalmus, P., Khan, R., Matone, L., & Márka, S. 2007, Class. Quant. Grav., 24, S659
Kaplan, D. L., Kulkarni, S. R., Frail, D. A., & van Kerkwijk, M. H. 2002, ApJ, 566, 378
Leahy, D. A., & Aschenbach, B. 1995, A&A, 293, 853
Mereghetti, S. 2008, A&AR, 15, 225
Owen, B. J. 2005, Phys. Rev. Lett., 95, 211101
Palmer, D., & Barthelmy, S. 2008, GCN Circ. 8115
Schwartz, S. J., et al. 2005, ApJ, 627, L129
Shapiro, S., & Teukolsky, S. 1983, Black Holes, White Dwarfs, and Neutron Stars (New York: Wiley)
Thompson, C., & Duncan, R. C. 1995, MNRAS, 275, 255
Thorne, K. S. 1987, in 300 Years of Gravitation, ed. W. Hawking & S. W. Israel (Cambridge: Cambridge Univ. Press), 417
Woods, P. M., & Thompson, C. 2004, in Compact Stellar X-Ray Sources, ed. W. G. H. Lewin & M. van der Klis (Cambridge: Cambridge Univ. Press)